Identification and characterization of the tungsten-containing class of benzoyl-coenzyme A reductases

Johannes W. Kung[a], Claudia Löffler[a], Katerina Dörner[b], Dimitri Heintz[c], Sébastien Gallien[d], Alain Van Dorsselaer[d], Thorsten Friedrich[b], and Matthias Boll[a,1]

[a]Institute of Biochemistry, University of Leipzig, 04103 Leipzig, Germany; [b]Institute of Biochemistry, University of Freiburg, 79104 Freiburg, Germany; [c]Institute de Biologie Moléculaire des Plantes, Centre National de la Recherche Scientifique (CNRS)-Unité Propre de Recherche 2357, Université de Strasbourg, 67083 Strasbourg, France; and [d]Laboratoire de Spectrométrie de Masse BioOrganique, IPHC-DSA, Institut Pluridisciplinaire Hubert Curien Département des Sciences Analytiques, Université de Strasbourg, CNRS, 67087 Strasbourg, France

Aromatic compounds are widely distributed in nature and can only be biomineralized by microorganisms. In anaerobic bacteria, benzoyl-CoA (BCoA) is a central intermediate of aromatic degradation, and serves as substrate for dearomatizing BCoA reductases (BCRs). In facultative anaerobes, the mechanistically difficult reduction of BCoA to cyclohexa-1,5-dienoyl-1-carboxyl-CoA (dienoyl-CoA) is driven by a stoichiometric ATP hydrolysis, catalyzed by a soluble, three [4Fe-4S] cluster-containing BCR. In this work, an in vitro assay for BCR from the obligately anaerobic *Geobacter metallireducens* was established. It followed the reverse reaction, the formation of BCoA from dienoyl-CoA in the presence of various electron acceptors. The benzoate-induced activity was highly specific for dienoyl-CoA ($K_m = 24 \pm 4\ \mu M$). The corresponding oxygen-sensitive enzyme was purified by several chromatographic steps with a 115-fold enrichment and a yield of 18%. The 185-kDa enzyme comprised 73- and 20-kDa subunits, suggesting an $\alpha_2\beta_2$-composition. MS analysis revealed the subunits as products of the benzoate-induced *bamBC* genes. The $\alpha\beta$ unit contained 0.9 W, 15 Fe, and 12.5 acid-labile sulfur. Results from EPR spectroscopy suggest the presence of one $[3Fe-4S]^{0/+1}$ and three $[4Fe-4S]^{+1/+2}$ clusters per $\alpha\beta$ unit; oxidized BamBC exhibited an EPR signal typical for a W(V) species. The FeS clusters and the W- cofactor could only be fully reduced by dienoyl-CoA. BamBC represents the prototype of a previously undescribed class of dearomatizing BCRs that differ completely from the ATP-dependent enzymes from facultative anaerobes.

anaerobic aromatic degradation | AOR | geobacter

Both naturally occurring and man-made aromatic compounds are ubiquitous and many are highly persistent and harmful to man and the environment. Only microorganisms are capable of fully degrading aromatic compounds to CO_2. Under aerobic conditions, bacteria use oxygenases to insert oxygen atoms into the ring to relieve ring resonance. In the absence of oxygen, this biochemical strategy is not an option, and anaerobic bacteria use completely different enzymes that relieve ring resonance by a reductive mechanism (1–4).

In anaerobic bacteria benzoyl-CoA (BCoA) is a central intermediate in the degradation pathways of many aromatic compounds. BCoA serves as the substrate for BCoA reductases (BCR), which dearomatize the aromatic ring by reduction yielding cyclohexa-1,5-diene-1-carboxyl-CoA (dienoyl-CoA; Fig. 1) (5–8). A BCR enzyme has so far only been isolated and studied in the denitrifying, facultative anaerobe *Thauera aromatica* (9). This extremely oxygen-sensitive enzyme has an $\alpha\beta\gamma\delta$-composition and harbors three $[4Fe-4S]^{+1/+2}$ clusters (10). It catalyzes electron transfer from reduced ferredoxin to the substrate with concomitant ATP hydrolysis (11), a reaction that was previously considered unique to nitrogenases (12). The coupling of electron transfer to an exergonic reaction is essential

to overcome the high redox barrier for aromatic ring reduction. Initial evidence for a mechanism via radical intermediates according to a Birch-type reduction has been obtained (13, 14).

Homologs of ATP-dependent BCRs from *T. aromatica* are present in the genomes of all facultative anaerobes described so far, which degrade low molecular aromatic growth substrates (5). In contrast, homologs of these genes are absent in the genomes of *Geobacter* species [Fe(III)-respiring] or *Syntrophus aciditrophicus* (fermenting), which are known to degrade benzoate (15–17). Also, the assay for ATP-dependent BCRs from facultative anaerobes failed with extracts from *Geobacter metallireducens* (16). The lack of an assay has so far prevented the study of an ATP independent BCR.

Recently, eight clustered benzoate-induced genes were identified, which are proposed to code for an uncharacterized BCR (Fig. 1B) (16). Homologs of this putative BamBCDEFGHI (BamB-I, encoded by gi78194549–41) complex (*bam*, benzoic acid metabolism) have so far only been identified in obligately anaerobic bacteria that use low molecular aromatic growth substrates. The individual proteins of the BamB-I complex show similarities to soluble components of NADH:quinone oxidoreductases (BamGHI), electron transfer components of hydrogenases (BamC and SeCys containing BamF), soluble heterodisulfide reductases (BamDE), and to Mo- or W-containing aldehyde:ferredoxin oxidoreductases (AORs, BamB). Accordingly, growth of two obligate anaerobes on benzoate depended on Mo or W and Se (16, 18). BamB was hypothesized to function as the active-site-containing component, whereas the remaining components were suggested to be involved in electron transfer from an unknown donor to BamB. Membrane proteome analysis of *G. metallireducens* revealed that at least the BamF and BamG components are membrane-associated (19). No ATP-binding motif was found in the BamB-I complex, suggesting that electron transfer to BCoA may be independent of ATP hydrolysis.

Here, we describe the isolation and characterization of the prototype of a new class of BCR enzymes. The catalytic components of this enzyme contain W and FeS clusters. The general features of the enzymes differ completely from that of known ATP-dependent BCRs even though the substrate and its product are identical.
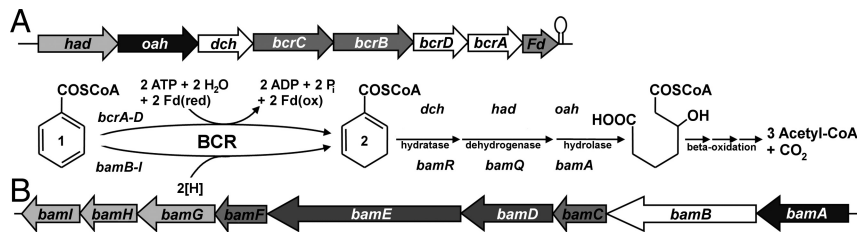
Fig. 1. Reaction of BCRs and organization of genes involved in BCoA degradation in *T. aromatica* and *G. metallireducens*. The BCoA degradation pathways proceed via identical intermediates in all anaerobic bacteria. All enzymes involved are highly similar in both organisms with the exception of BCR involved in the reduction of BCoA (1) to dienoyl-CoA (2). (*A*) Cluster of genes coding for BCR (*bcrA-D*) and other enzymes (*had*, *oah*, and *dch*) of the BCoA degradation pathway in *T. aromatica*. Note that BcrA-D couples ring reduction to a stoichiometric ATP hydrolysis (upper BCR reaction). (*B*) Cluster of genes coding for putative BCR (*bamB-I*) and another enzyme (*bamA*, a homolog for *oah*) involved in the BCoA degradation pathway in *G. metallireducens*. For simpler presentation, the *bamRQ* genes are not shown. The reaction catalyzed by BamB-I is suggested to be ATP independent (lower BCR reaction).

Results

Enzyme Assay for BCR from *G. metallireducens*. To date, in vitro enzyme activities have only been determined for ATP-dependent BCRs from facultative anaerobes using low-potential artificial electron donors (9). Although indirect evidence was provided that BCoA reduction should yield dienoyl-CoA in all anaerobes (8), the assay failed with extracts derived from obligate anaerobes grown on an aromatic growth substrate (16). To circumvent the dependence on an electron-activating system for the forward reaction, we determined the reverse reaction, the electron acceptor-dependent oxidation of dienoyl-CoA. This reaction is driven by aromatization and should be highly exergonic in the presence of appropriate electron acceptors. The dienoyl-CoA used throughout this study was enzymatically synthesized from BCoA using purified BCR from *T. aromatica* (20).

Soluble extracts from *G. metallireducens* cells grown on benzoate catalyzed the time-, protein-, and dienoyl-CoA-dependent reduction of 2,6-dichlorophenol indolphenol (DCPIP) in a pseudofirst order reaction as determined in a spectrophotometric assay. HPLC analysis of samples taken at different time points confirmed the formation of BCoA from dienoyl-CoA (a representative HPLC assay with the purified enzyme is shown in Fig. S1). One DCPIP was reduced per BCoA formed. The dienoyl-CoA oxidizing activity was oxygen-sensitive (for details, see below). For this reason, all steps were carried out under strictly anoxic conditions; DCPIP could not be replaced by oxygen as electron acceptor. Because the dienoyl-CoA aromatizing activity was sensitive to dilution (<0.1 mg mL^{-1}), the enzyme assay routinely contained 5 mg mL^{-1} BSA. The activity was present in extracts of cells grown on benzoate (400–600 nmol min^{-1} mg^{-1}), but was virtually absent in extracts from cells grown on acetate (<1 nmol min^{-1} mg^{-1}). Addition of MgATP or MgADP (5 mM each) had no effect on the activity. After ultracentrifugation, 45% of the dienoyl-CoA oxidizing activity was found in the membrane fraction. Addition of 500 mM KCl to the extract buffer released 95% of the aromatizing activity into the soluble protein fraction. After ultracentrifugation and a desalting step, the soluble protein fraction was used for purification.
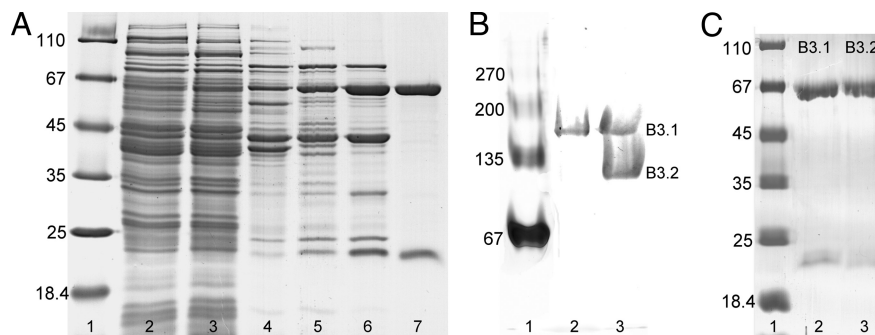
Purification of Dienoyl-CoA:Acceptor Oxidoreductase. With the spectrophotometric assay established, the isolation of the dienoyl-CoA aromatizing enzyme was carried out. Purification was accomplished in five chromatographic steps, including DEAE-Sepharose anion exchange chromatography (elution at 225 mM KCl at pH 7.8), Cibacron Blue and Reactive Red affinity chromatography (flow through, respectively), hydroxyapatite chromatography (elution at 80 mM sodium phosphate at pH 7.8), and Source Q anion exchange chromatography (elution at 210 mM KCl at pH 7.8). The order of columns used and the integration of the two affinity chromatography steps were essential for complete removal of contaminants. A typical purification protocol is shown in Table 1. A 115-fold enrichment with a yield of 18% was achieved. From 20 g cells (wet mass), ≈6 mg protein with a specific activity of 68 μmol min^{-1} mg^{-1} were obtained.

Molecular Properties, Genes, and Cofactors of the Dienoyl-CoA Aromatizing Enzyme. SDS/PAGE analysis of the enzyme fractions obtained during the purification procedure revealed the enrichment of protein bands migrating at 65 and 20 kDa in an almost 1:1 ratio after normalization for the molecular masses (Fig. 2*A*). The excised bands were analyzed by nanoliquid chromatography-coupled tandem MS (nanoLC-MS/MS) after enzymatic digestion with trypsin. By using MASCOT MS/MS data searches against *G. metallireducens* protein database, the resulting peptides were identified to belong to the *bamC* gene product (gi78194548, 52% sequence coverage, 20-kDa subunit) and to the *bamB* gene product (gi78194549, 60% sequence coverage, 65-kDa subunit; for MS data, see Table S1). Therefore, the dienoyl-CoA oxidizing enzyme is henceforth termed BamBC. The masses as deduced from the amino acid sequences of BamB and BamC were 73 and 21 kDa, respectively. The discrepancy between the molecular masses of BamB as deduced from the amino acid sequence (73 kDa) and as determined by SDS PAGE (65 kDa) is unclear. The peptides identified by MS did not indicate a loss of a corresponding 8-kDa peptide at the C or N terminus. BamBC had a native molecular mass of 185 ± 10 kDa as determined by gel filtration, suggesting an $\alpha_2\beta_2$ composition.

Table 1. Protocol for purification of BamBC

Purification step	Volume, mL	Total activity, U	Protein, mg	Specific activity, U mg^{-1}	Yield, %	Enrichment, fold
100,000 × *g* supernatant	79	1,778	2,955	0.6	100	1.0
Dialysis	80	2,102	2,880	0.7	118	1.2
DEAE	310	1,273	322	3.9	71	6.6
CibacronBlue/ReactiveRed	320	615	102	6.0	35	10
Hydroxyapatite	50	452	22	20	26	33
SourceQ	24	321	6.0	68	18	115

One U refers to the oxidation of 1 μmol min^{-1} dienoyl-CoA. Activities were determined with DCPIP as electron acceptor.

Fig. 2. Purification of BamBC and activity staining. A SDS-polyacrylamide gel of dienoyl-CoA:acceptor oxidoreductase activity containing fractions obtained during the purification of BamBC from *G. metallireducens*, 7 μg of protein per lane. Lane 1, molecular mass standard; lane 2, cell extract; lane 3, dialysed extract; lane 4, DEAE Sepharose; lane 5, Cibacron Blue and Reactive Red agarose; lane 6, hydroxyapatite; lane 7, SourceQ Sepharose. (*B*) Native gel electrophoresis and activity staining. Lane 1, BSA standard (Coomassie-stained); lane 2, soluble extract of cells grown benzoate; lane 3, purified BamBC. Lanes 2 and 3 were activity-stained. (*C*) SDS polyacrylamide gel analysis of bands activity-stained bands (B3.1 and B3.2). Lane 1, molecular mass standard; lane 2, excised band at 180 kDa in *B*; lane 3, excised band at 100 kDa in *B*.

Purified BamBC was subjected to native gel electrophoresis. Subsequent activity staining with dienoyl-CoA as electron donor, DCPIP as primary and a staining redox dye as secondary electron acceptor revealed two protein bands of ≈180 and 100 kDa (Fig. 2*B*). Both bands were excised and analyzed by denaturing gel electrophoresis. In both cases two bands migrating at the corresponding molecular masses of BamB and BamC were obtained; the assignment of the proteins bands to BamBC was confirmed by MS analysis. Thus, the two bands obtained after native gel electrophoresis apparently represent the $\alpha_2\beta_2$ and $\alpha\beta$ forms of BamBC (Fig. 2*C*). In extracts from cells grown on benzoate, only one band ≈180 kDa was obtained on native gels after activity staining (Fig. 2*B*). Obviously, in cell extracts, BamBC was more resistant to dissociation during native gel electrophoresis than in the as-isolated form.

The amount of iron and acid labile sulfur per mol $\alpha\beta$-unit was 15.2 ± 0.6 mol Fe and 12.7 ± 1.4 mol acid labile sulfur as determined colorimetrically (mean values ± SDs). Inductively coupled plasma (ICP) MS analysis of metals and Se revealed the presence of 0.9 W, 1.2 Zn, and 2.1 Ca per $\alpha\beta$ unit; the amount of Mn, Co, Ni, Cu, V, Se, and Mo was <0.05 mol per mol $\alpha\beta$ unit.

Factors Affecting BamBC Activity. BamBC as isolated in the absence of a reducing agent had a half life in air of ≈3 h. Sensitivity was greatly enhanced to a half-life <30 s when the enzyme was incubated with dithionite or dienoyl-CoA before oxygen exposure. Under anoxic conditions in the oxidized state, it was stable at −20 °C for weeks in the presence of 5% PEG$_{4000}$. Virtually no loss of activity was observed when BamBC was incubated with 5 mM sodium cyanide for up to 2 h at 4 °C.

UV/vis and EPR Spectroscopy. The dark brownish enzyme as isolated was considered to be in the oxidized state. It exhibited a typical UV/vis spectrum of iron-sulfur proteins with a shoulder between 400 and 450 nm (Fig. 3*A*). Virtually complete reduction of BamBC (1–5 μM) was accomplished by excess of dienoyl-CoA (50 μM). In contrast, addition of sodium dithionite (50 μM) bleached the spectrum of oxidized BamBC only by 10% when compared with dienoyl-CoA. The difference spectrum (oxidized minus dienoyl-CoA reduced form) exhibited a maximum at 409 nm (Fig. 3*A*, *Inset*); the molecular extinction coefficients as determined are presented in Table 2.

Oxidized BamBC as isolated showed two distinct EPR signals (Fig. 3 *B* and *C*). They are indicative for S = 1/2 signals of a [3Fe-4S]$^{+1}$ cluster (optimally developed at 10 K) and a W(V) species (40 K). At higher temperatures, the W(V) signal changed from an axial (g_x = 1.893, g_y = g_z = 1.986) to a rhombic signal

(g_z = 2.013). On addition of excess dienoyl-CoA, both signals disappeared. In parallel complex and very broad, fast relaxing signals optimally developed at 10 K and 20 mW spanning >70 mT. The signal is interpreted as a mixture of interacting and noninteracting low-spin [4Fe-4S]$^+$ clusters. The features between 330 and 370 mT showed nearly identical power saturation and temperature dependencies, which did not allow the extraction of subspectra from single species. On addition of dithionite, the [3Fe-4S]$^{+1}$ signal disappeared, whereas the W(V) signal remained, although at lower intensity. In agreement with UV/vis spectroscopy, the [4Fe-4S] clusters were hardly reducible to the paramagnetic +1-state by dithionite. In accordance to metal analysis, one BamBC is suggested to contain a W$^{+4/+5/+6}$-cofactor, one [3Fe-4S]$^{+1/0}$, and three [4Fe-4S]$^{+1/+2}$ clusters.

Substrate Preference and Kinetic Properties. BamBC was highly specific for 1,5-dienoyl-CoA. None of the following dienoyl-CoA/monoenoyl-CoA analogs was converted as tested by HPLC analysis: 1,3-dienoyl-CoA, 1,4-dienoyl-CoA, 1-enoyl-CoA, 2-enoyl-CoA, and 3-enoyl-CoA (0.2 mM each). Benzaldehyde, crotonaldehyde, and acetaldehyde were not oxidized (2 mM each), and they had no inhibitory effect on dienoyl-CoA oxidation. BamBC used the electron acceptors benzyl viologen (350%
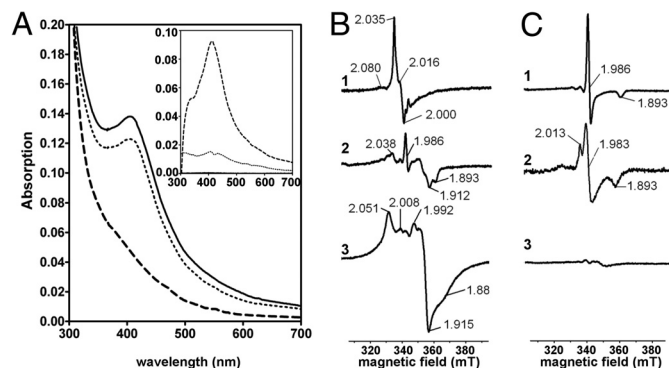
Fig. 3. UV/vis and EPR spectroscopy of BamBC. (*A*) UV/vis spectra of BamBC (*Inset*, difference spectra): solid line, as isolated (1 μM); dotted line, reduced with dithionite (50 μM); and dashed line, reduced with 1,5-dienoyl-CoA (50 μM). (*B*) Selected EPR spectra of FeS clusters at optimal conditions: B1, as isolated at 10 K, 20 mW after subtraction of spectrum C1; B2, dithionite reduced at 20 K, 5 mW; and B3 dienoyl-CoA reduced at 10 K, 20 mW. C EPR spectra of W(V): C1, as isolated at 40 K, 5 mW; C2, as isolated at 80 K, 5 mW; and C3, dienoyl-CoA reduced at 40 K, 5 mW. The numbers refer to *g* values. All EPR spectra were recorded at 0.6 mT modulation amplitude.

BIOCHEMISTRY

Table 2. Properties of BamBC

Property	Value
Reaction catalyzed	Dienoyl-CoA + acceptor$_{ox}$ → Benzoyl-CoA + acceptor$_{red}$
Native molecular mass	185 $\pm$ 10 kDa
Subunits	BamB (73 kDa), BamC (21 kDa)
Molecular composition	$\alpha_2\beta_2$
Cofactor content (per $\alpha\beta$)	W: 0.9 Ca: 2.1 Zn: 1.2
	Fe 15.2 $\pm$ 0.6
	Acid labile S: 12.7 $\pm$ 1.4
UV/vis absorption maxima	oxidized: $\varepsilon_{280} = 290{,}000$ M^{-1} cm^{-1}
	oxidized: $\varepsilon_{417} = 82{,}500$ M^{-1} cm^{-1}
	oxidized–reduced: $\varepsilon_{409} = 44{,}900$ M^{-1} cm^{-1}
K_m (dienoyl-CoA)	24 $\pm$ 4 μM
Catalytic no.	52 s^{-1} (per $\alpha\beta$)
Half-life on air	30 s (reduced), 3 h (oxidized)

activity) and methyl viologen (360% activity) at higher rates than DCPIP (100% activity, 0.4 mM each). In all cases, a stoichiometry of two electrons transferred per dienoyl-CoA oxidized was observed. BamBC did not catalyze the reduction of BCoA using Ti-(III)-citrate (5 mM), sodium dithionite (1 mM), or reduced methyl viologen (0.5 mM) as electron donors. BamBC was active in a broad pH range from 5 to 9 with an optimum at pH 6.8. The initial rates of the reaction followed Michaelis–Menten kinetics with an apparent K_m for dienoyl-CoA of 24 $\pm$ 4 μM (mean value $\pm$ SD). The presence of BCoA had virtually no inhibitory effect on the initial rate at concentrations up to 0.5 mM by using 0.1 mM dienoyl-CoA.

Discussion

Properties of BamBC and Assignment to a Previously Undescribed Class of BCoA Reductases. In this work, the prototype of a previously undescribed class of tungsten containing BCR enzymes was identified and characterized (properties are summarized in Table 2). Although the forward reaction could not be followed with BamBC in the absence of the electron activation components, the following properties support the contention that BamBC indeed represent the active site components of BCR from *G. metallireducens*. (*i*) The reaction was highly specific for dienoyl-CoA, whereas none of the other dienoyl-CoA/monoenoyl-CoA isomers tested was converted. (*ii*) Only dienoyl-CoA, but not the artificial reductant dithionite, completely reduced the enzyme as determined by UV/vis and EPR spectroscopy. (*iii*) Both transcription of the *bamBC* genes (16), as well as the dienoyl-CoA aromatizing activity were highly induced by an aromatic growth substrate. (*iv*) Highly similar homologs of the *bamBC* genes are present only in strict anaerobes that degrade aromatic compounds (Fig. 4). (*v*) The identification of W as cofactor fits well with the recently identified benzoate-induced tungstate transporter (19).

EPR spectroscopy and sequence comparisons with similar enzymes indicate that BamB represents the tungstopterin and [4Fe-4S] cluster-containing active site component, whereas BamC represents a two [4Fe-4S] and a [3Fe-4S] cluster-containing electron transfer subunit (16). The BamB subunit shows high amino acid sequence similarities (45–90%) identities to homologues from other *Geobacter* and *Syntrophus* species, and up to 30% identity to AOR-like enzymes from organisms that do not use aromatic growth substrates (16). Phylogenetic analysis suggests that BamB enzymes represent a separate class within the AOR family (Fig. 4). AORs usually catalyze the oxidation of aldehydes to the corresponding carboxylic acids, and the electrons are transferred to ferredoxin (21, 22). Because BamBC did not oxidize any of the tested aldehydes, the biological functions of AORs and BamBC appear to differ fundamentally.

In the case of BamBC, an unusual role of the tungsten cofactor is proposed as tungsto- or molybdo-pterin enzymes usually catalyze oxygen atom transfer reactions (23). The W(V) low spin EPR signal only disappeared on dienoyl-CoA addition supporting its catalytic relevance. Like other AOR enzymes, BamBC contained Ca, which is involved in pterin cofactor binding (24). The presence of Zn and an additional Ca in BamBC is rather unusual; both may function as Lewis acids for the stabilization of negatively charged radical/nonradical intermediates.

BamBC used the low potential electron acceptor methyl viologen without reaching thermodynamic equilibrium, suggesting that the E°′ of the BCoA/dienoyl-CoA redox couple is far < -500 mV (E°′ methyl viologen$_{ox/red} = -448$ mV) (25). The low potential can be rationalized by the largely exergonic aromatization reaction, and explains why dienoyl-CoA, but not dithionite, was capable of fully reducing BamBC.

The BamBC components of *G. metallireducens* BCR share no similarities to the known ATP-dependent BCRs from facultative
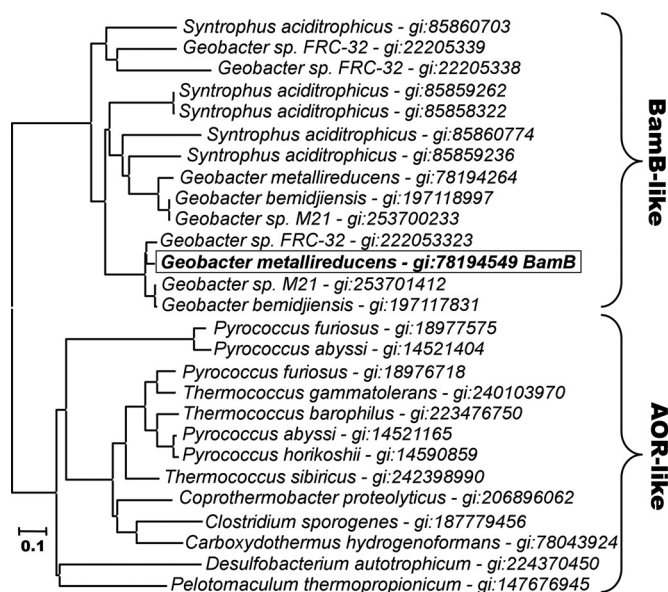
Fig. 4. Phylogenetic analysis of BamB and other AOR-like enzymes. The amino acid sequences used in the BamB cluster derive from the genomes of *Geobacter* and *Syntrophus* species that are known to degrade aromatic compounds. Note that many paralogs may be present in one organism. The sequences of AORs depicted are those with the highest similarities to BamB genes. For phylogenetic analysis (maximum likelihood method) the Mega4 software package was used (http://www.megasoftware.net/).

anaerobes. Obviously, the capability of dearomatizing BCoA has evolved twice in nature in two completely different ways.

The BamD-I components are hypothesized to constitute a complex electron transfer system that acts in conjunctions with BamBC. Obviously, they are not tightly attached to BamBC and are not required for dienoyl-CoA oxidation. BamD-I are predicted to contain numerous additional FeS clusters, two flavins and a SeCys (16).

Possible Scenarios for the Forward Reaction of BCR from *G. metallireducens*. BCRs are suggested to dearomatize the aromatic ring in a Birch-like reduction reaction via single electron transfer steps. The assumed extremely low redox potential for the first electron transfer requires an activation reaction. There are two plausible scenarios for ATP-independent electron activations in BCR from *G. metallireducens*.

A previous membrane proteome analysis revealed benzoate-induced proteins with similarities to components of energy-converting hydrogenases (19). The proteins lack the Ni-containing active site domain, which excludes a role in a hydrogenase reaction. Instead, they could represent attractive components involved in a membrane potential-driven electron transfer to BamBC via the BamDEFGHI modules. Alternatively, an electron bifurcation may drive the unfavorable electron transfer to the aromatic ring. This process was originally described for an electron transferring flavoprotein containing two FAD cofactors. It coupled the exergonic electron transfer from NADH to crotonyl-CoA to the endergonic one from NADH to ferredoxin (26, 27). The flavin cofactors were considered essential for this bifurcation of electrons. Notably, amino acid sequence comparisons suggested that BamE and BamH both contain flavin-binding motifs (16). However, by using various combinations of electron donors/acceptors, no evidence for such a bifurcation could be obtained (see *Materials and Methods*). It has to be considered that, even under very mild extract preparation conditions, BamBC activity was always distributed in both the soluble and membrane protein fraction. Also, BamD-I did not copurify. In summary, cell rupture obviously destroyed the correct assembly of the electron activation machinery. A screening for more stable BamB-I variants in other obligate anaerobes is required to overcome these problems in the future.

Materials and Methods

Cultivation of Cells and Preparation of Extracts. *G. metallireducens* (DSMZ 7210) was anaerobically cultivated in a 200-L-fermenter at 30 °C in a mineral salt medium (28) with benzoate (5 mM) or acetate (30 mM) as sole carbon source and nitrate (15 mM) as electron acceptor. For the preparation of crude extracts, frozen cells were anaerobically suspended at 4 °C in 20 mM triethanolamine/HCl, 5 mM MgCl₂, pH 7.8 (referred to as buffer A, 2 mL g⁻¹ cell, wet mass), containing 500 mM KCl, 0.02 mg DNase I, and 0.02 mg dithioerythritol. Cell disruption was accomplished by alternate freezing in liquid nitrogen and thawing (three times). The $100,000 \times g$ pellet (1 h at 4 °C) was washed in buffer A containing 150 mM KCl (1 mL g⁻¹ wet cells) and centrifuged again. Combined supernatants were used for further studies.

Synthesis of CoA Esters. BCoA was synthesized from benzoic acid anhydride and CoA (29). Dienoyl-CoA was enzymatically synthesized from BCoA by using enriched BCR from *T. aromatica*; the product was purified by preparative HPLC as described (7). Other CoA-esters were synthesized as described earlier (20).

Enzyme Assays. All assays were carried out in anaerobically sealed cuvettes at 30 °C under a N₂ atmosphere (100%). Dienoyl-CoA:acceptor oxidoreductase activity was determined based of the absorbance change of DCPIP during reduction ($\Delta\varepsilon_{700}$ = 5,900 M⁻¹ cm⁻¹ at pH 7.3, self-determined). The assay mixture (400 μL) contained 150 mM Mops/KOH, 15 mM MgCl₂, 150 mM NaCl, 5 mg mL⁻¹ BSA pH 7.3 (referred to as buffer B), plus 0.4 mM DCPIP, 0.2 mM dienoyl-CoA, and 1–10 μg of protein. Alternatively, benzyl viologen (ε_{578} = 12,000 M⁻¹ cm⁻¹) or methyl viologen (ε_{730} = 2,400 M⁻¹ cm⁻¹) (30) were used as electron acceptors in the spectrophotometric assay. In the discontinuous

assay (400 μL), 25 μL samples were taken at different time points and analyzed by HPLC as described (20). This assay was used for product analysis.

To test the forward reaction in cell extract preparations, Ti(III)-citrate (5 mM), dithionite (5 mM), and reduced methyl viologen (1 mM) were used as electron donors. As ferredoxin reducing system 2-oxoglutarate (5 mM) plus CoA (0.5 mM) were used. For potential electron bifurcation reactions NAD(P)⁺ (1 mM), and menadione (0.2 mM) were combined with all of the donors listed above.

Purification of BamBC. All steps were performed at 4 °C in an anaerobic glove box (N₂:H₂, 95:5, by vol.). Extracts of 20 g cells (wet mass) were dialysed overnight against 2.5-L buffer A containing 150 mM KCl. The $3,500 \times g$ supernatant (80 mL) was applied to a DEAE-Sepharose column (Fast Flow, volume 100 mL, diameter 5.1 cm; GE Healthcare), which had been equilibrated with buffer A. The column was washed at a flow rate of 6 mL min⁻¹ with 3 bed vol of buffer A, followed by 5 bed vol of 120 mM NaCl in buffer A. Activity was eluted in a step gradient at 225 mM NaCl in buffer A within 310 mL. The fractions containing activity were applied onto Cibacron Blue Agarose 3GA Type 3000-CL (volume, 50 mL; diameter, 5.1 cm; Sigma–Aldrich) and Reactive Red Agarose 120 Type 3000-CL (volume, 30 mL; diameter, 2.6 cm; Sigma–Aldrich) columns connected directly to each other at a flow rate of 4 mL min⁻¹; both columns had been equilibrated with 150 mM NaCl in buffer A. Activity was obtained in the flow-through (320 mL). The pooled fraction were applied to a hydroxyapatite column (MacroPrep, ceramic hydroxyapatite 40 μm, 30 mL, 2.6 diameter; BioRad) at a flow rate of 4 mL min⁻¹ equilibrated with buffer A. The column was washed with 3 bed volumes of 20 mM potassium phosphate pH 7.8; activity eluted in a step gradient at 80 mM potassium phosphate, pH 7.8 (50 mL). For the last purification step, a Source 15Q column (HiLoad, volume 8 mL, 1.6 cm diameter; GE Healthcare) was equilibrated with buffer A containing 150 mM NaCl (flow rate 2 mL min⁻¹). The fractions applied eluted in a linear 150–300 mM NaCl gradient (50 bed volumes) at ≈210 mM NaCl. The dienoyl-CoA:acceptor oxidoreductase activity containing fractions were concentrated in microconcentrators (30-kDa exclusion limit, Vivaspin 6; Sartorius) by centrifugation. The enzyme solution was slowly diluted under gentle stirring with a 20% (wt/vol) PEG₄₀₀₀ stock solution in buffer B to a final concentration of 5% (wt/vol) and kept frozen in anaerobic glass vials at −20 °C. In this form, the enzyme was stable for several weeks.

Determination of Molecular Mass. Native mass of BamBC was determined by analytical gel filtration via Superdex 200 (10/300 GL column, GE Healthcare; 25 mL column volume; 0.5 mL min⁻¹ flow rate) using 20 mM triethanolamine-HCl buffer, pH 7.8, 4 mM MgCl₂, 150 mM KCl. The column was calibrated with apoferritin (443 kDa), catalase (245 kDa), BSA (67 kDa), and carboanhydrase (29 kDa).

Determination of Metal Cofactors and Acid-Labile Sulfur. The content of iron and acid labile sulfur was determined colorimetrically by the methods of Lovenberg (31) and Beinert (32), respectively. W, Mo, V, Zn, Ca, Cu, Ni, Co, Mn, and Se were determined by ICP-MS analysis at the Helmholtz Centre for Environmental Research, Leipzig, Germany (Wennrich, Division for Analytics and Ecotoxicology). To exclude metal contamination, the last purification step (Source 15Q) was carried out by using chemicals of the highest purity available (RotiPuran Water, Roth; NaCl and NaOH TraceSelect grade, Sigma–Aldrich, respectively). The amount of metals and selenium in a protein-free buffer sample control was negligible.

Determination of Kinetic Properties and Oxygen Sensitivity. For K_m determination, the dienoyl-CoA concentration was varied from 3 to 200 μM by fitting the initial rates to Michaelis–Menten curves using the Prism software package (GraphPad). For determination of the pH dependence of the reaction, buffer B was supplemented by sodium acetate and Tris/HCl (0.15 M each). For oxygen inactivation assays, the enzyme was gently stirred in air at 4 °C, an anaerobically incubated enzyme served as control. The spectrophotometric assay was started by enzyme addition after different incubation times. To test the effect of cyanide (5 mM), the enzyme was anaerobically incubated at 4 °C for different time intervals before the assays were started (2 h). The substrate preference was tested with dienoyl-CoA/monoenoyl-CoA analogs at 0.2 mM concentrations; aldehydes as indicated were tested at 2 mM concentrations.

MS Analysis of BamBC. Gel bands of interest were digested *in gel* with trypsin and peptides were extracted as described previously (33). The resulting peptide were analyzed by nanoLC-MS/MS on an Agilent 1100 Series HPLC-Chip/MS system (Agilent Technologies) coupled to an HCT Ultra ion trap (Bruker Daltonics) for the SDS/PAGE analysis of the enzyme fraction, or on a nanoAC-QUITY Ultra-Performance-LC (UPLC, Waters) coupled to SYNAPT hybrid quad-

rupole orthogonal acceleration time-of-flight tandem mass spectrometer (Waters) for the SDS/PAGE analysis of the bands obtained after native gel analysis. The MS/MS data were analyzed using the MASCOT 2.2.0. algorithm (Matrix Science) to search against an in-house generated target-decoy protein database from *G. metallireducens*.

UV/vis Spectroscopy. UV/vis spectra of purified BamBC (1–5 μM in buffer B without BSA) were recorded with a UV-1650PC Shimadzu spectrophotometer in a gas-tight quartz cuvette under anaerobic conditions. Dithionite (0.05 mM) or dienoyl-CoA (0.05 mM) were added from anaerobic stock solutions in buffer without BSA.

EPR Spectroscopy. EPR measurements were conducted with a Bruker EMX 1/6 spectrometer operating at X-band. The sample temperature was controlled with an Oxford instrument ESR-9 helium flow cryostat. The magnetic field was calibrated using a strong or a weak pitch standard. Samples were taken from the BamBC as isolated (300 μM in buffer A plus 5% PEG$_{4000}$, wt/vol), and after

1 min incubation with 4 mM dithionite or by 4.6 mM of dienoyl-CoA. EPR conditions were: microwave frequency, 9.44 GHz; modulation amplitude, 0.6 mT; time constant, 0.164 s; scan rate, 17.9 mT min^{-1}.

Further Determinations. SDS/PAGE (12.5%) was carried out according to Laemmli. Proteins were visualized using SimplyBlue SafeStain (Invitrogen). Protein was routinely determined by the method of Bradford using BSA as standard. Native gel electrophoresis and activity staining were carried out as described (20). Briefly, it followed the dienoyl-CoA-dependent reduction of 3-(4′,5′-dimethylthiazol-2-yl)-2,4-diphenyltetrazolium bromide in the presence of DCPIP. Excised bands were incubated at 95 °C in 20 μL SDS sample buffer for 10 min and analyzed by SDS/PAGE (12.5% wt/vol).

1. Boll M, Fuchs G, Heider J (2002) Anaerobic oxidation of aromatic compounds and hydrocarbons. *Curr Opin Chem Biol* 6:604–611.
2. Carmona M, et al. (2009) Anaerobic catabolism of aromatic compounds: A genetic and genomic view. *Microbiol Mol Biol Rev* 73:71–133.
3. Fuchs G (2008) Anaerobic metabolism of aromatic compounds. *Ann NY Acad Sci* 1125:82–99.
4. Gibson J, Harwood CS (2002) Metabolic diversity in aromatic compound utilization by anaerobic microbes. *Annu Rev Microbiol* 56:345–369.
5. Boll M (2005) Dearomatizing benzene ring reductases. *J Mol Microbiol Biotechnol* 10:132–142.
6. Boll M (2005) Key enzymes in the anaerobic aromatic metabolism catalysing Birch-like reductions. *Biochim Biophys Acta* 1707:34–50.
7. Boll M, et al. (2000) Nonaromatic products from anoxic conversion of benzoyl-CoA with benzoyl-CoA reductase and cyclohexa-1,5-diene-1-carbonyl-CoA hydratase. *J Biol Chem* 275:21889–21895.
8. Peters F, Shinoda Y, McInerney MJ, Boll M (2007) Cyclohexa-1,5-diene-1-carbonyl-coenzyme A (CoA) hydratases of *Geobacter metallireducens* and *Syntrophus aciditrophicus*: Evidence for a common benzoyl-CoA degradation pathway in facultative and strict anaerobes. *J Bacteriol* 189:1055–1060.
9. Boll M, Fuchs G (1995) Benzoyl-coenzyme A reductase (dearomatizing), a key enzyme of anaerobic aromatic metabolism. ATP dependence of the reaction, purification and some properties of the enzyme from *Thauera aromatica* strain K172. *Eur J Biochem* 234:921–933.
10. Boll M, Fuchs G, Meier C, Trautwein A, Lowe DJ (2000) EPR and Mossbauer studies of benzoyl-CoA reductase. *J Biol Chem* 275:31857–31868.
11. Boll M, Albracht SS, Fuchs G (1997) Benzoyl-CoA reductase (dearomatizing), a key enzyme of anaerobic aromatic metabolism. A study of adenosinetriphosphatase activity, ATP stoichiometry of the reaction and EPR properties of the enzyme. *Eur J Biochem* 244:840–851.
12. Buckel W, Hetzel M, Kim J (2004) ATP-driven electron transfer in enzymatic radical reactions. *Curr Opin Chem Biol* 8:462–467.
13. Thiele B, Rieder O, Golding BT, Müller M, Boll M (2008) Mechanism of enzymatic Birch reduction: Stereochemical course and exchange reactions of benzoyl-CoA reductase. *J Am Chem Soc* 130:14050–14051.
14. Mobitz H, Boll M (2002) A Birch-like mechanism in enzymatic benzoyl-CoA reduction: A kinetic study of substrate analogues combined with an ab initio model. *Biochemistry* 41:1752–1758.
15. McInerney MJ, et al. (2007) The genome of *Syntrophus aciditrophicus*: Life at the thermodynamic limit of microbial growth. *Proc Natl Acad Sci* 104:7600–7605.
16. Wischgoll S, et al. (2005) Gene clusters involved in anaerobic benzoate degradation of *Geobacter metallireducens*. *Mol Microbiol* 58:1238–1252.
17. Butler JE, et al. (2007) Genomic and microarray analysis of aromatics degradation in Geobacter metallireducens and comparison to a Geobacter isolate from a contaminated field site. *BMC Genomics* 8:180.
18. Peters F, Rother M, Boll M (2004) Selenocysteine-containing proteins in anaerobic benzoate metabolism of *Desulfococcus multivorans*. *J Bacteriol* 186:2156–2163.
19. Heintz D, et al. (2009) Membrane proteome analysis reveals novel benzoate induced proteins in *G. metallireducens*. *Mol Cell Prot* 8:2159–2169.
20. Thiele B, et al. (2008) Aromatizing cyclohexa-1,5-diene-1-carbonyl-coenzyme A oxidase. Characterization and its role in anaerobic aromatic metabolism. *J Biol Chem* 283:20713–20721.
21. Chan MK, Mukund S, Kletzin A, Adams MW, Rees DC (1995) Structure of a hyperthermophilic tungstopterin enzyme, aldehyde ferredoxin oxidoreductase. *Science* 267:1463–1469.
22. Roy R, Menon AL, Adams MW (2001) Aldehyde oxidoreductases from *Pyrococcus furiosus*. *Methods Enzymol* 331:132–144.
23. Hille R (2005) Molybdenum-containing hydroxylases. *Arch Biochem Biophys* 433:107–116.
24. Hu Y, Faham S, Roy R, Adams MW, Rees DC (1999) Formaldehyde ferredoxin oxidoreductase from Pyrococcus furiosus: The 1.85 Å resolution crystal structure and its mechanistic implications. *J Mol Biol* 286:899–914.
25. Wardman P (1989) Reduction potentials of one-electron couples NADH-dye reductase and a non-haem iron protein involving free radicals in aqueous solution. *J Phys Chem Ref Data* 18:1637–1755.
26. Herrmann G, Jayamani E, Mai G, Buckel W (2008) Energy conservation via electron-transferring flavoprotein in anaerobic bacteria. *J Bacteriol* 190:784–791.
27. Li F, et al. (2008) Coupled ferredoxin and crotonyl coenzyme A (CoA) reduction with NADH catalyzed by the butyryl-CoA dehydrogenase/Etf complex from *Clostridium kluyveri*. *J Bacteriol* 190:843–850.
28. Lovley DR, et al. (1993) Geobacter metallireducens gen. nov. sp. nov., a microorganism capable of coupling the complete oxidation of organic compounds to the reduction of iron and other metals. *Arch Microbiol* 159:336–344.
29. Schachter D, Taggart JV (1953) Benzoyl coenzyme A and hippurate synthesis. *J Biol Chem* 203:925–934.
30. White H, Strobl G, Feicht R, Simon H (1989) Carboxylic acid reductase: A new tungsten enzyme catalyses the reduction of non-activated carboxylic acids to aldehydes. *Eur J Biochem* 184:89–96.
31. Lovenberg W, Buchanan BB, Rabinowitz JC (1963) Studies on the chemical nature of clostridial ferredoxin. *J Biol Chem* 238:3899–3913.
32. Beinert H (1983) Semi-micro methods for analysis of labile sulfide and of labile sulfide plus sulfane sulfur in unusually stable iron-sulfur proteins. *Anal Biochem* 131:373–378.
33. Gallien S, et al. (2009) Ortho-proteogenomics: Multiple proteomes investigation through orthology and a new MS-based protocol. *Genome Res* 19:128–135.